Effects of Single-Base Bulges on Intercalator Binding to Small RNA and DNA Hairpins and a Ribosomal RNA Fragment†

Susan A. White‡ and David E. Draper*
Department of Chemistry, The Johns Hopkins University, Baltimore, Maryland 21218
Received August 29, 1988; Revised Manuscript Received October 27, 1988

ABSTRACT: The way in which a single-base bulge might affect the structure of an RNA helix has been examined by preparing a series of six RNA hairpins, all with seven base pairs and a four-nucleotide loop. Five of the hairpins have single-base bulges at different positions. The intercalating cleavage reagent (methidiumpropyl)-EDTA–Fe(II) [MPE–Fe(II)] binds preferentially at a CpG sequence in the helix lacking a bulge and in four of the five hairpins with bulges. Hairpins with a bulge one or two bases to the 3′ side of the CpG sequence bind ethidium 4–5-fold more strongly than the others. V1 RNase, which is sensitive to RNA backbone conformation in helices, detects a conformational change in all of the helices when ethidium binds; the most dramatic changes, involving the entire hairpin stem, are in one of the two hairpins with enhanced ethidium affinity. Only a slight conformational change is detected in the hairpin lacking a bulge. A bulge adjacent to a CpG sequence in a 100-nucleotide ribosomal RNA fragment enhances MPE–Fe(II) binding by an order of magnitude. These results extend our previous observations of bulges at a single position in an RNA hairpin [White, S. A., & Draper, D. E. (1987) *Nucleic Acids Res. 15*, 4049] and show that (1) a structural change in an RNA helix may be propagated for several base pairs, (2) bulges tend to increase the number of conformations available to a helix, and (3) the effects observed in small RNA hairpins are relevant to larger RNAs with more extensive structure. A bulge in a DNA hairpin identical in sequence with the RNA hairpins does not enhance MPE–Fe(II) binding affinity, relative to a control DNA hairpin. The effects of bulges on ethidium intercalation are evidently modulated by helix structure.

The secondary structures of several large RNAs are now understood in some detail, largely as a result of extensive phylogenetic studies (Noller, 1984; Michel & Dujon, 1983; James et al., 1988). A frequently conserved structural motif in these RNAs is an extra unpaired nucleotide, or single-base bulge, within certain helices. In several instances deletion of a bulged nucleotide affects binding of a protein (Christiansen et al., 1985; Wu & Uhlenbeck, 1987; C. Tang and D.E.D., unpublished observations), but the role of bulges in protein recognition or other RNA functions is largely unknown. We have therefore been interested in studying the structural consequences of introducing a single-base bulge into an RNA helix.

In previous work, we noticed that the affinity–cleavage reagent MPE–Fe(II)[1] intercalates with unusually high affinity at a CpG sequence in a large fragment of the 16S rRNA (Kean et al., 1985). A single-base bulge lies to the 3′ side of this site. Studies of ethidium and MPE–Fe(II) binding to a set of small RNA hairpins duplicating seven base pairs of the rRNA sequence showed that (1) a single-base bulge may enhance ethidium binding at the CpG sequence by an order of magnitude, (2) A, C, and U bulges all have identical effects, and (3) ethidium intercalation induces a concerted change in the conformation of the entire helix when the bulge is present but only perturbs the helix structure locally at the CpG site in the absence of a bulge (White & Draper, 1987). These results show that the presence of an extra sugar–phosphate unit in the backbone allows the RNA to adopt an alternate conformation normally inaccessible to the helix and suggest a possible functional role for bulges in large RNAs.

In this paper we ask what effect the bulge position within the helix has on intercalator binding and on any conformational transition. We also show that the effects of bulges we see in small hairpins are reproduced in a much larger rRNA fragment.

Experimental Procedures

Preparation of Plasmid Clones. Construction of plasmids containing the T7 RNA polymerase promoter sequence followed by DNA coding for the *Escherichia coli* 16S ribosomal RNA nucleotides 648–753 is described in Draper et al. (1988a). [Numbering of the 16S rRNA bases is from the 5′ terminus (Brosius et al., 1980).] Briefly, a *Hin*dIII–*Hae*III DNA fragment covering nucleotides 649–734 of the 16S rRNA was cloned into pT7-2 (U.S. Biochemicals) along with an 8-bp *Sma*I linker, $d(C_4G_4)$. A synthetic DNA duplex reproducing the 16S rRNA nucleotides 735–753 and containing an *Eco*RV restriction site was then ligated between the plasmid *Sma*I and *Sac*I sites to give the plasmid pHRV2. When this plasmid is cut with *Eco*RV and transcribed with T7 RNA polymerase, the runoff transcripts have the sequence (5′ to 3′) pppGGGAGACCGG-[16S nucleotides 648–753]-U_{OH}. By synthesizing alternate DNA oligomers, modified sequences having a deletion of nucleotide A746 (pHRV4) or a substitution of a U at position 746 (pHRV6) were made.

RNA Synthesis. The small hairpins were synthesized by transcribing partially single stranded DNA templates with T7 RNA polymerase (Milligan et al., 1987; Draper et al., 1988a). The RNA was purified by electrophoresing the transcription reaction through a denaturing gel (20% acrylamide, 50% urea) and cutting out individual bands detected by UV shadowing. The RNA was extracted from the gel, end-labeled with cytidine [^{32}P]bisphosphate and T4 RNA ligase, and repurified

† This work was supported by NIH Grant GM37005. D.E.D. is the recipient of an NIH Research Career Development Award (CA01081), and S.A.W. was supported in part by a fellowship from the American Association of University Women Educational Foundation.

‡ Present address: Department of Chemistry, Yale University, P.O. Box 6666, New Haven, CT 06511-8118.

[1] Abbreviation: MPE, (methidiumpropyl)-EDTA.

0006-2960/89/0428-1892$01.50/0

on a second denaturing gel as previously described (Kean et al., 1985). The rRNA fragments were transcribed from the plasmid DNAs described above; *Eco*RV was used to linearize the plasmids. The RNA from these transcriptions were first purified by gel filtration on a Superose 12B column (Pharmacia) and then end-labeled and repurified on 12% acrylamide denaturing gels in the same way as the small hairpins. The transcription conditions are described in Draper et al. (1988a). T7 RNA polymerase was purified from the overproducing strain BL21(pAR1219) (Danvaloo et al., 1984).

Each of the hairpins synthesized was completely sequenced by partial RNase digestion of hairpins 3′-end-labeled with ^{32}P. T_1 RNase was obtained from Boehringer Mannheim, and the other nucleases were from BRL. T_1 (G specific), U_2 (A, G specific), and Phy M (U, A specific) RNases were used in 7 M urea, 25 mM sodium citrate, pH 5, and 1 mM EDTA, at 55 °C. With *Bacillus cereus* RNase (U, C specific) the urea was omitted, and with CL3 RNase (C specific) 10 mM sodium phosphate, pH 6.5, was substituted for the sodium citrate. Since the hairpins are quite stable, it was difficult to digest base-paired nucleotides, and several concentrations of enzyme were used with each sequence. Transcription of each DNA template yielded many spurious transcripts in addition to the expected product. These included hairpins missing the bulged base (see Results) and, in the U14 RNA, hairpins with insertions of extra nucleotides in the U_4 loop.

The bulgeless and C16 hairpins were transcribed in the presence of [α-^{32}P]GTP and the internally labeled RNAs completely digested with T_1 RNase. After electrophoresis on a 20% acrylamide gel, five fragments of the sizes expected were obtained in each case. Any significant misincorporation at G nucleotide positions would have resulted in additional, larger fragments.

DNA Hairpins. DNAs were synthesized by using *O*-methylphosphoramidite chemistry on an Applied Biosystems synthesizer. After deblocking, 200 pmol of a DNA hairpin were 3′-end-labeled by incubation for 1 h at 37 °C in 10 μL containing 140 mM sodium cacodylate, pH 7.2, 1 mM cobalt chloride, 0.1 mM dithiothreitol, 50 μCi of [α-^{32}P]dideoxyATP (Amersham), and 30 units of terminal nucleotidal transferase (BRL). The labeled product was gel-purified in the same way as the RNA hairpins.

MPE–Fe(II) and V1 Reactions. MPE–Fe(II) reactions were carried out as described previously, in 5-μL total volume (Kean et al., 1985). The reactions included 10 mM Tris, pH 7.6, 100 mM NaCl, and 2 mM DTT to initiate the cleavage and were incubated at 37 °C for 20 min. At the end of the incubation, 5 μL of urea buffer (10 M urea, 20 mM EDTA, 0.1% xylene cyanol dye) was added and the reaction placed on ice just prior to electrophoresis. The free MPE–Fe(II) concentration was adjusted by adding poly(A)-poly(U), and the added RNA also helps stabilize the methidium moiety against radical reactions. The total MPE–Fe(II) concentration was usually either 2 or 10 μM, depending on the binding constant range being measured. V1 nuclease (Pharmacia) reactions with RNA hairpins were carried out in the same way as for the MPE–Fe(II) reactions but included 1 mM $MgCl_2$ required for nuclease activity. DNase I (Sigma, type II) reactions were carried out in 100 mM Tris, pH 7.6, 10 mM $MgCl_2$, and 0.01–1 unit of enzyme. Serial dilutions of ethidium bromide were used to titrate the reactions.

The reactions were electrophoresed through 0.4 mm thick 20% acrylamide–50% urea gels containing 0.1 M Tris base, 0.1 M boric acid, and 1 mM Na_2EDTA. Each gel was run with a control reaction, alkaline hydrolysis, and T_1 RNase

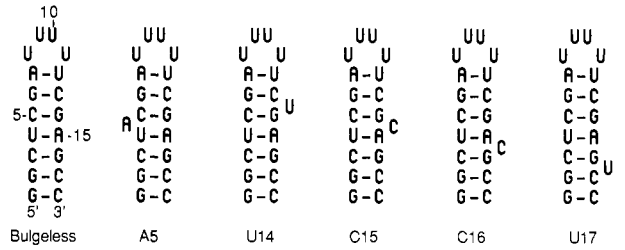

FIGURE 1: RNA hairpins prepared by in vitro transcription for this study. The RNAs all retain the 5′-terminal triphosphate (not shown). The hairpins containing bulges are named after the bulged base and its position in the sequence.

digestion carried out under denaturing conditions for reference. For the DNA hairpins, the G-specific reaction with dimethyl sulfate was run for reference (Maxam & Gilbert, 1980).

The concentrations of hairpins in the reactions were less than 0.03 μM. At these low concentrations the sequences ran as monomeric hairpins in nondenaturing gels; even at $\approx$0.2 μM we found no evidence for bimolecular complexes.

Data Analysis. Autoradiograms of gels were scanned with a Joyce-Loebl Chromoscan 3 densitometer. Free MPE–Fe(II) concentrations were calculated from the experimentally determined binding isotherm for MPE–Fe(II) binding poly(A)-poly(U) (Kean et al., 1985; White, 1988). (The concentration of hairpin was always small compared to the free MPE–Fe(II) concentration and did not enter into the calculations.) Plots of peak intensity vs MPE–Fe(II) concentration were fit to hyperbolic binding isotherms by using a least-squares protocol (Draper et al., 1988b); both the equilibrium binding constant and the maximum peak intensity are allowed to vary to give an optimum fit. For any one hairpin, binding curves derived from several different peaks representing cleavages at different nucleotides in the RNA were usually analyzed and always gave similar results. The binding constants reported are averages of at least three independent sets of reactions.

Results

Synthesis of Small Hairpins Containing Single-Base Bulges. A series of RNA hairpins containing seven base pairs, a four-nucleotide loop, and a single-base bulge at various positions in the helix were synthesized (Figure 1). Four base pairs of the hairpin (CUCG–CGAG) duplicate part of a 16S rRNA helix (nucleotides 558–661 and 744–748) and contain the CpG sequence originally observed to have an unusually high affinity for intercalators (Kean et al., 1985). The hairpins were synthesized by transcription from partially single stranded DNA templates (Milligan et al., 1987; Draper et al., 1988). A significant fraction of the transcription products were closely related RNAs approximately twice the expected length. The polymerase also tended to "skip" the bulged base in the hairpin sequence, and the "bulgeless" hairpin was frequently the single most abundant transcription product. These artifacts were probably due to very stable secondary structure in the DNA template and are discussed further by Draper et al. (1988a). The correct transcript was identified by thorough enzymatic sequencing in each case (see Experimental Procedures).

Site of MPE–Fe(II) Intercalation. MPE–Fe(II) binding at a unique site within a helix sequence produces a set of cleavages that are staggered to the 3′ side of the intercalation site on either strand, because of the right-handed geometry of the helix and the location of the Fe(II)–EDTA complex in the helix minor groove. MPE–Fe(II) cleavage of an RNA hairpin with 9 bp showed two sets of cleavages offset to the 3′ side of the sequence CpG, and ethidium-induced cleavage

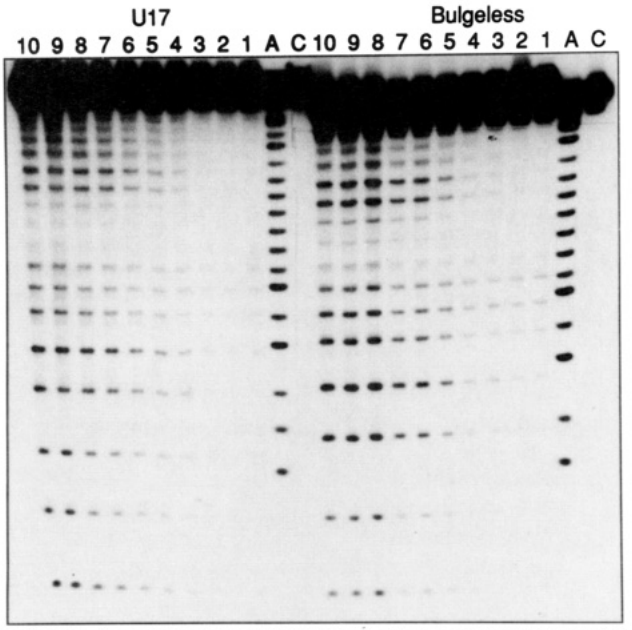

FIGURE 2: Autoradiograms from gel electrophoresis of hairpins reacted with MPE–Fe(II). (Lane C) Control lane with no MPE–Fe(II); (lane A) alkaline hydrolysis; (lanes 1–10) reaction with free MPE–Fe(II) concentrations of 0.24, 0.56, 0.78, 1.5, 2.1, 3.8, 4.7, 6.4, 8.1, and 9.0 μM, respectively. [The total MPE–Fe(II) concentration was 10 μM in each lane; see Experimental Procedures.] The set of reactions on the left is with the U17 hairpin, and the bulgeless hairpin is on the right.

Table I: MPE–Fe(II) Affinity for Various RNA and DNA Helices[a]

binding site	K (μM^{-1})	binding site	K (μM^{-1})
RNAs		HRV2	3.35 ± 0.8
bulgeless	0.46 ± 0.15	HRV4	0.42 ± 0.15
bulge U14	0.60 ± 0.2	HRV6	4.3 ± 0.8
bulge C15	2.5 ± 0.8		
bulge C16	2.1 ± 0.5	DNAs	
bulge U17	0.50 ± 0.2	bulgeless	0.43 ± 0.1
bulge A5	0.63 ± 0.15	bulge dC15	0.55 ± 0.1

[a] Binding constants reported are the averages of three or more independent measurements. See Experimental Procedures for details.

of the RNA upon irradiation at 514 nm confirmed that the CpG sequence is a unique intercalation site in the hairpin (White & Draper, 1987). The smaller, 7-bp hairpins shown in Figure 1 are related in sequence to the 9-bp hairpin previously studied, and we expected MPE–Fe(II) to give a similar cleavage pattern. This is the case for most of the hairpins. Figure 2 is an autoradiogram obtained after electrophoresis of an MPE–Fe(II) reaction, and Figure 3 summarizes the cleavage data from several different hairpins. The 9- and 7-bp hairpins clearly have very similar cleavage patterns. All of the hairpins shown in Figure 1 gave similar results, with the exception of A5, which shows no clearly defined peak of cutting intensity along the helix backbone (Figure 3C). All of the cleavage sites titrate in parallel with MPE–Fe(II) concentration, and cleavage at all the sites is reduced by competing ethidium bromide (not shown). We conclude that MPE–Fe(II) binds to two or more sites in the A5 hairpin with comparable affinity, while the remaining hairpins all bind MPE–Fe(II) at the CpG sequence preferentially.

MPE–Fe(II) Affinity for RNA Hairpins. From the extent of hairpin cutting with increasing MPE–Fe(II) concentration (Figure 2), equilibrium binding constants can be calculated (see Experimental Procedures). Plots derived from densitometer scans of two titrations are shown in Figure 4, and binding constants for the entire set of hairpins are listed in Table I. Most of the hairpins bind MPE–Fe(II) with an

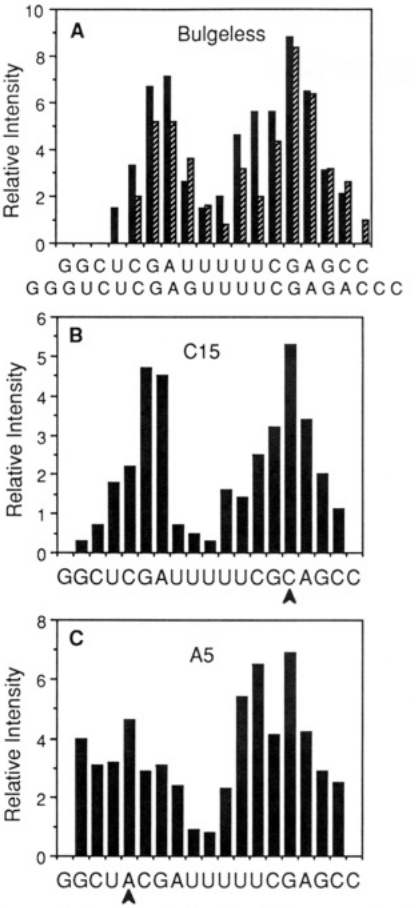

FIGURE 3: Extent of cleavage obtained at different nucleotide positions after reaction of hairpins with MPE–Fe(II). The extent of cutting is expressed in arbitrary units. (A) Reaction of either the bulgeless helix shown in Figure 1 with 3.7 μM MPE–Fe(II) (top sequence and solid bars) or the longer 9-bp hairpin described in White and Draper (1987) (bottom sequence and hatched bars). (B) Reaction of hairpin C15 with 1.0 μM MPE–Fe(II). (C) Reaction of hairpin A5 with 1.9 μM MPE–Fe(II). Arrowheads indicate the extra, bulged nucleotide in (B) and (C).

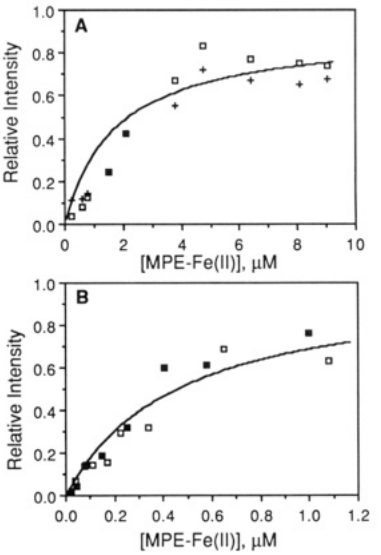

FIGURE 4: Titrations of hairpins with MPE–Fe(II). (A) Bulgeless helix; extents of cleavage at nucleotide G6 (□) or C13 (+) from the same reaction are shown. The solid line is the predicted titration for a binding constant of 0.57 μM^{-1}. (B) Hairpin C15. The two symbols are from two independent reactions, and the line is calculated for a binding affinity of 2.2 μM^{-1}.

affinity of ≈0.5 μM^{-1}, but C15 and C16 both have affinities 4–5-fold higher.

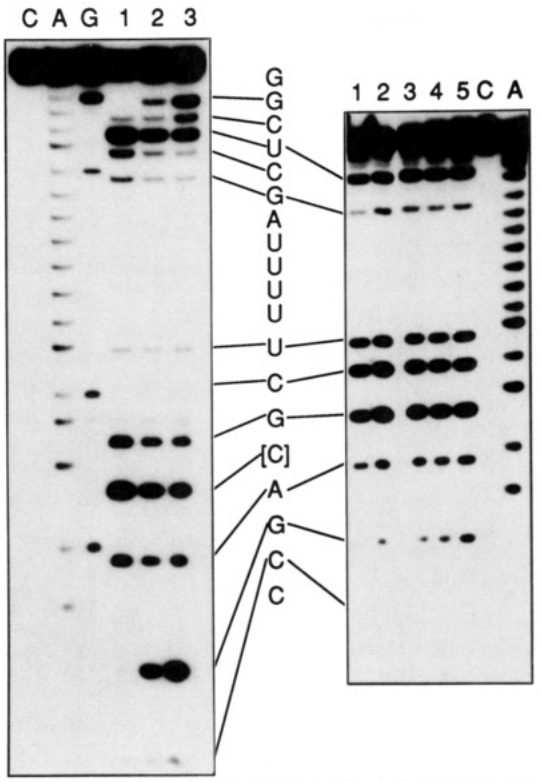

FIGURE 5: Autoradiogram from gel electrophoresis of RNA hairpins digested with V1 RNase in the presence of ethidium bromide. (Left) C15 hairpin digested with 0, 2.2, and 4.4 μM ethidium present (lanes 1–3, respectively). (Right) Bulgeless hairpin digested with 0, 2.2, 4.4, 8.8, or 17.6 μM ethidium (lanes 1–5, respectively). In each panel, lane C represents a control lane (no V1 RNase); (lane A) alkaline hydrolysis; (lane G) partial T1 RNase digestion under denaturing conditions.

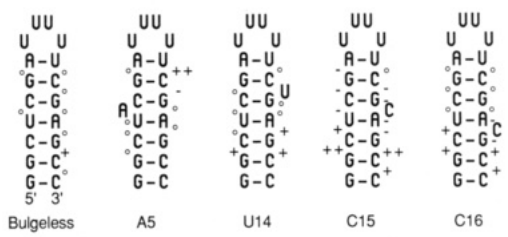

FIGURE 6: Summary of changes in V1 RNase cleavage rates with RNA hairpins in response to ethidium binding. (○) Phosphodiester is cleaved but shows no significant change in reactivity with ethidium present; (+ or −) V1 RNase cleavage rate is enhanced (+) or decreased (−) by less than a factor of 2 when ethidium is added; (++) V1 RNase cleavage is enhanced by more than a factor of 2.

Effects of Ethidium Binding on V1 Digestion Patterns. The V1 RNase from cobra venom is sensitive to the RNA backbone conformation, and preferentially hydrolyzes helical RNA (Lowman & Draper, 1985). To see if intercalation at the CpG sequence affects the conformation of any of the hairpins, we looked at each hairpin V1 RNase digestion pattern in the presence of several ethidium bromide concentrations. The results are shown in Figures 5 and 6. The bulgeless hairpin shows only a minor change in V1 reactivity at a single position, while C15 shows changes in reactivity at almost every base pair step in the helix. Enhancements in reactivity at G2 and G17 are particularly dramatic. V1 nuclease senses some conformational changes in the remaining hairpins, but they are less extensive than those detected in the C15 hairpin. Competition experiments show that ethidium binds to these hairpins about 3-fold more weakly than does MPE–Fe(II) (not shown), so the ethidium concentration range needed to detect changes in V1 reactivity is the same required for intercalation at the CpG site.

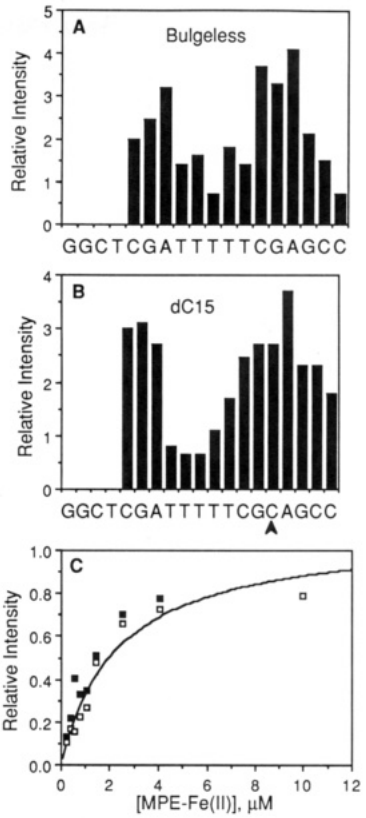

FIGURE 7: MPE–Fe(II) cleavage of DNA hairpins. (A) Extent of cleavage with the bulgeless DNA hairpin. (B) Extent of cleavage with the dC15 hairpin. (C) Titration of the bulgeless (■) or dC15 (□) hairpins. The solid line is calculated for a binding constant of 0.44 μM^{-1}.

MPE–Fe(II) Reactions with DNA Hairpins. The RNA hairpins described here presumably have the A-form helix conformation. DNA, under the conditions of our experiments, is more likely to be in the B form. It was therefore interesting to see whether the effects of bulges that we observe in RNA hairpins are reproduced in DNA hairpins; if these effects depend on details of base stacking interactions and backbone configurations, then quite different results might be obtained. The DNA equivalents of the bulgeless and C15 hairpins were synthesized; their reactivities toward MPE–Fe(II) are shown in Figure 7 and their affinities for MPE–Fe(II) listed in Table I. Nucleotides to the 3′ sides of the CpG sequence again tend to be the most intensely cut, especially in the bulgeless helix. In the dC15 hairpin, the envelope of cuts is rather broad and suggests that significant binding at other dinucleotide steps besides dCpdG is taking place. The presence of a bulge has virtually no effect on the MPE–Fe(II) binding affinity.[2]

V1 RNase does not digest DNA, so we attempted to detect any helix conformational changes with DNase I instead (data not shown). Only four cleavage sites were observed: two strong sites following nucleotides dG6 and dG14 and weaker

[2] The MPE–Fe(II) hairpin affinities listed in Table I have been measured by titration with an excess of MPE–Fe(II). Only the highest affinity binding site in a hairpin is detected, and the binding measurement is unaffected if multiple sites are present in the RNA. Therefore, a bulge may increase the number of intercalation sites in a hairpin (i.e., enhance binding at very weak sites) without changing the binding constant measurement. It is likely that both the A5 and dC15 hairpins have an increased number of intercalation sites (relative to the bulgeless hairpin), even though they do not show an increased affinity for MPE–Fe(II).

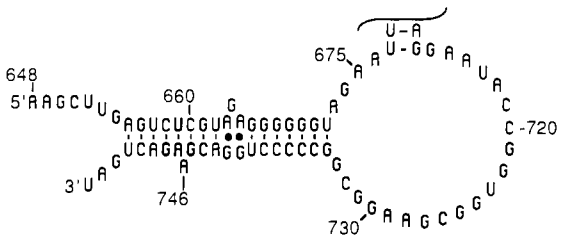

FIGURE 8: Sequence and secondary structure of a portion of the HRV4 ribosomal RNA fragment. Numbering is the same as in intact 16S rRNA, and the base pairing is the phylogenetically conserved secondary structure (Noller, 1984).

cutting at dA7 and dA15 (bulgeless) or dC15 (dC15 hairpin). The cleavage rates in either helix were unaffected by the addition of ethidium up to 10 μM. Since so few sites are cleaved by the DNase, it is not possible to decide whether or not conformational changes occur within the helices.

MPE-Fe(II) Binding to Larger rRNA Fragments. Having found that single-base bulges may affect the affinity of ethidium or MPE intercalators for small RNA hairpins, we wished to see if the same would be true for much larger RNAs with more complex secondary and tertiary structures. We had previously found five clusters of cuts in a 345-nucleotide fragment from the central domain of the 16S rRNA. These cuts are the result of particularly high affinity MPE-Fe(II) binding and are probably due to binding at two separate sites in the RNA (Kean et al., 1985). Two sets of cuts are centered around G661 and A746 (see Figure 8) and probably reflect intercalation at a helix CpG sequence adjacent to the bulged A746. (The other three sets of cuts are near G671, G727, and C735.) We prepared RNA fragments covering nucleotides 648–753 of the 16S ribosomal RNA with the wild-type sequence, with a substitution of a U for A746 and with a deletion of A746. Titrations of these RNAs with MPE-Fe(II) are shown in Figure 9, and binding constants are listed in Table I. It is clear that the bulge does enhance intercalation at the CpG sequence in this larger RNA. MPE-Fe(II) cleavage at the remaining three clusters of cuts is unaffected by the bulged base (not shown), confirming that there are at least two independent sites with high affinity for MPE-Fe(II) in this RNA domain.

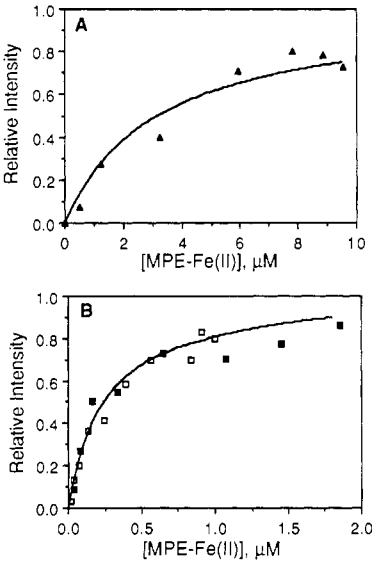

FIGURE 9: Titrations of the HRV RNAs with MPE-Fe(II). (A) Titration of HRV4 (ΔA746) RNA; the solid line is calculated for a binding affinity of 0.36 μM^{-1}. Cleavage at G745 is plotted. (B) Titration of HRV2 (A746) (□) or HRV4 (U746), (■) RNAs; the solid line is calculated for a binding affinity of 4.2 μM^{-1}. Cleavage after nucleotide 746 is plotted in each case.

Discussion

Effects of Bulges on RNA Helices. We can summarize our observations of the effects of single-base bulges on RNA hairpins in two statements. First, a bulge is able to influence the intercalation of ethidium bromide one or two base pairs distant. Streisinger et al. (1966) originally speculated that ethidium would bind preferentially at the site of a single-base bulge, since the bulge would allow the backbone to extend more easily. However, the U14 hairpin shows that a bulge does not necessarily affect intercalation at the same site. An indirect mechanism is required to explain the effects of the C15 and C16 bulges on ethidium binding; presumably the bulge affects the structure of the helix in a way that facilitates intercalation or stabilizes the ethidium–helix complex.

The second statement we can make is that intercalation at a single site in an RNA helix may affect the helix backbone structure (as detected by V1 RNase) several base pairs distant. This effect depends on the presence of a bulge in the helix; with both a 9-bp hairpin (White & Draper, 1987) and the 7-bp hairpin described here, intercalation has almost no effect on the V1 RNase digestion pattern in the absence of a bulge. The position of the bulge in the helix determines how extensive and intense the effects are; only the C15 hairpin shows changes in structure throughout the helix. Extensive structural changes do not correlate with higher ethidium affinity, since the C16 and U14 hairpins show only small changes in V1 reactivity confined to half of the helix, even though their affinities for ethidium are significantly different.

These observations, together with our previous studies of single-base bulges, lead us to conclude that RNA helices must be able to respond to a structural change (i.e., ethidium intercalation) over at least several base pairs and in some situations are able to undergo essentially allosteric conformational changes. In these hairpins, single-base bulges seem to strongly facilitate changes to alternate conformations. There is some evidence that RNA helices can transmit structural changes in the absence of bulges. A recent study by Seong and RajBhandary (1987) has shown that the conformation and function of the anticodon loop in initiator $tRNA^{fmet}$ are dependent on the correct sequence of G-C and C-G base pairs within the anticodon stem, and there is considerable evidence that codon–anticodon interactions in tRNA are coupled to changes in tertiary structure via the anticodon stem (Rigler & Wintermeyer, 1983).

Bulges Have Similar Effects in Small Hairpins and in Larger RNAs. An important result for the functional relevance of our studies is the finding that a conserved single-base bulge in a ribosomal RNA fragment has roughly the same effect on MPE-Fe(II) binding as it does in small hairpins. The bulge and intercalation site are embedded in a much more extensive helical region in the rRNA fragment (Figure 8), so the effects we observe are not dependent on having a small stem–loop structure. It seems likely that ribosomes and other ribozymes require conformational changes during their catalytic cycles, and a functional role for single-base bulges in RNAs may be to permit the RNA to switch between different conformations. Even minor changes in twisting or bending of an RNA helix could have profound effects on tertiary interactions in a large RNA.

Propagation of Structural Changes in RNA Helices. How can ethidium intercalation at the CpG sequence influence helix conformation several base pairs distant? Of the four variables used to describe the conformation of a helix (slide, roll, helical

twist, and propeller twist), changes in only slide and propeller twist can be propagated cooperatively through the helix (Dickerson, 1983; Calladine & Drew, 1984). CpG sequences in A-form helices tend to have either unusually high propeller twist (Dickerson, 1983) or unusually large slide brought about by an all-trans backbone conformation (Haran et al., 1987; Heinemann et al., 1987). A single-crystal structure of ethidium intercalated in CpG shows almost no propeller twist and a slightly negative slide (Jain et al., 1977). Thus, intercalation has the potential for changing the conformations of the two C-G base pairs in a way that would be communicated to neighboring base pairs.

Our results suggest that single-base bulges make cooperative changes in base-pair conformation energetically more favorable, though mechanisms by which this might take place are difficult to visualize in detail. Since A, C, and U bulges have identical effects on ethidium intercalation (White & Draper, 1987), the extra sugar–phosphate moiety is probably the important feature, rather than the base itself. In a regular helix changes in the backbone or glycosyl torsion angles of a nucleotide on one strand tend to produce the opposite change in the opposing strand (Drew et al., 1981; Dickerson, 1983). A bulge, by introducing an extra backbone unit, may weaken this coupling and allow each strand of a helix to adopt a greater range of conformations. We clearly need much more structural information about base-pair and backbone conformations in RNA helices to begin to understand the mechanisms underlying these conformational transitions.

Single-Base Bulges in DNA. The DNA helices we studied differed from the RNA hairpins of identical sequence in two ways: the DNA shows less specificty for intercalation at the CpG site, and a single-base bulge has no effect on the intercalator affinity (though there may be some effect on the number of intercalation sites). Calladine and Drew (1984) have argued that A- and B-form helices use fundamentally different strategies to maximize base stacking at pyrimidine–purine sequences: the tendency in B-form DNA is for stacking to occur between bases in the same strand, while RNA (or A-form DNA) uses interstrand stacking. Therefore, the conformation of the CpG sequence might be quite different between RNA and DNA, and ethidium intercalation will influence the CpG and neighboring base-pair conformations in different ways.

Two studies have detected an influence of bulges on intercalation in short DNA helices. Nelson and Tinoco (1985) found an order of magnitude increase in ethidium affinity when a bulged C is inserted in the middle of a $(dA)_6$ tract. dA-dT tracts are now known to have an unusually high propeller twist and a bifurcated hydrogen bonding scheme that would be disrupted by ethidium binding (Nelson et al., 1987). The bulge may destabilize this hydrogen bonding and lower the thermodynamic cost of intercalation. In another study, a bulge was placed at seven different sites in a DNA dodecamer, and MPE–Fe(II) cutting was slightly enhanced in the vicinity of the bulge in each case (Williams & Goldberg, 1988). Certainly, bulges in DNA may influence intercalation, but one should expect DNA and RNA to respond differently.

Thermodynamics of Helix Conformational Changes. Single-base bulges enhance ethidium binding by a factor of 4 or 5 in the 7-bp hairpins, and by an order of magnitude in a 9-bp hairpin (White & Draper, 1987). This factor sets an upper limit of $\approx$0.8 kcal on the free energy required to induce a switch to the alternate hairpin conformation. This energy is small compared to the total van der Waals stacking energy stabilizing helices (Haran et al., 1984) and may represent subtle changes in the overlap of base pairs. Since very little conformational change is detected in the bulgeless helix, the implication is that this RNA sequence is confined to one conformation, unable to make extensive conformational readjustments without significant thermodynamic cost.

Registry No. A5, 118334-10-4; U14, 118334-06-8; C15, 118334-08-0; C16, 118334-09-1; U17, 118334-07-9; CpG, 2382-65-2; MPE–Fe(II), 83789-87-1; ethidium bromide, 1239-45-8; bulgeless, 118334-04-6; 648–753 of 16S rRNA, 118334-26-2.

References

Brosius, J., Dull, T. J., & Noller, H. F. (1980) *Proc. Natl. Acad. Sci. U.S.A. 77*, 201–205.

Calladine, C. R., & Drew, H. R. (1984) *J. Mol. Biol. 178*, 773–782.

Christiansen, J., Douthwaite, S. R., Christensen, A., & Garrett, R. (1985) *EMBO J. 4*, 1019–1024.

Danvaloo, P., Rosenberg, A. H., Dunn, J. J., & Studier, F. W. (1984) *Proc. Natl. Acad. Sci. U.S.A. 81*, 2035–2039.

Dickerson, R. E. (1983) *J. Mol. Biol. 166*, 419–441.

Draper, D. E., White, S. A., & Kean, J. M. (1988a) *Methods Enzymol.* (in press).

Draper, D. E., Deckman, I. C., & Vartikar, J. V. (1988b) *Methods Enzymol.* (in press).

Drew, H. R., Wing, R. M., Takano, T., Broka, C., Tanaka, S., Itakura, K., & Dickerson, R. (1981) *Proc. Natl. Acad. Sci. U.S.A. 78*, 2179–2183.

Haran, T. E., Berkovich-Yellin, Z., & Shakked, A. (1984) *J. Biomol. Struct. Dyn. 2*, 397–412.

Haran, T. E., Shakked, Z., Wang, A. H.-J., & Rich, A. (1987) *J. Biomol. Struct. Dyn. 5*, 199–217.

Heinemann, U., Lauble, H., Frank, R., & Blöker, H. (1987) *Nucleic Acids Res. 15*, 9531–9549.

Jain, S. C., Tsai, C., & Sobell, H. M. (1977) *J. Mol. Biol. 114*, 317–331.

James, B. D., Olsen, G. J., Liu, J., & Pace, N. R. (1988) *Cell 52*, 19–26.

Kean, J. M., White, S. A., & Draper, D. E. (1985) *Biochemistry 24*, 5062–5070.

Lowman, H. B., & Draper, D. E. (1986) *J. Biol. Chem. 261*, 5396–5403.

Maxam, A., & Gilbert, W. (1980) *Methods Enzymol. 65*, 497–559.

Michel, F., & Dujon, B. (1983) *EMBO J. 2*, 33–38.

Milligan, J. F., Groebe, D. R., Witherell, G. W., & Uhlenbeck, O. C. (1987) *Nucleic Acids Res. 15*, 8783–8798.

Nelson, J. W., & Tinoco, I. (1985) *Biochemistry 24*, 6416–6423.

Nelson, H. C. M., Finch, J. T., Luisi, B. F., & Klug, A. (1987) *Nature 330*, 221–226.

Noller, H. F. (1984) *Annu. Rev. Biochem. 53*, 119–162.

Rigler, R., & Wintermeyer, W. (1983) *Annu. Rev. Biophys. Bioeng. 12*, 475–505.

Seong, B. L., & RajBhandary, U. L. (1987) *Proc. Natl. Acad. Sci. U.S.A. 84*, 334–338.

Streisinger, G., Okada, Y., Emrich, J., Newton, J., Tsugita, A., Tzeraghi, E., & Inouye, M. (1966) *Cold Spring Harbor Symp. Quant. Biol. 31*, 77–84.

White, S. A. (1988) Ph.D. Thesis, Johns Hopkins University.

White, S. A., & Draper, D. E. (1987) *Nucleic Acids Res. 15*, 4049–4064.

Williams, L. D., & Goldberg, I. H. (1988) *Biochemistry 27*, 3004–3011.

Wu, H.-N., & Uhlenbeck, O. C. (1987) *Biochemistry 26*, 8221–8227.